Effects of Dipole Orientations on Nonlinear Optical Properties of Oxo-Bridged Dinitroaniline Systems

Ayan Datta and Swapan K. Pati*

Theoretical Sciences Unit and Chemistry and Physics of Materials Unit, Jawaharlal Nehru Center for Advanced Scientific Research, Jakkur Campus, Bangalore 560 064, India

Received: June 30, 2003; In Final Form: October 1, 2003

We have considered several oxo-bridged dinitroaniline compounds in various dipole configurations. An extensive semiempirical calculations based on singles configuration interactions (CIS) was performed to calculate their nonlinear optical properties. While keeping one of the nitroaniline dipole moieties fixed, we rotate the other nitroaniline molecule along the oxygen−carbon bond to generate a number of dipole orientations. We also change the position of the donor−acceptor functionalities from ortho and meta to para and study the variation in the nonlinear optical properties with the twist angle. We find that the best conformation is where the nitroaniline dipoles are arranged parallel to each other in the same plane. In real systems steric interaction between the two aromatic rings would force the double molecule to be nonplanar. We suggest molecular systems where the moieties can be made parallel, thereby exhibiting very high hyperpolarizabilities. We interpret these results on the basis of dipole−dipole interactions and the ground-state properties.

1. Introduction

Materials with large second harmonic coefficients are of huge current interest. Devices made up of these materials are finding a large number of applications in various disciplines, from lasers to optical switches and electronics.[1]

Conjugated organic molecules have a lot of potential to be used as good nonlinear optical materials.[2] These molecules have delocalized π electrons over a large length scale of the molecule, which can be very easily manipulated by substitution of electron donating (push) and electron withdrawing (pull) groups around the aromatic moieties. Apart from structural flexibility, which allows fine-tuning of chemical structures and properties for the desired nonlinear optical properties,[3−5] the organic materials are of great technological interest because of their low cost, ease of fabrication, and integration into devices.

Recently, a series of oxygen-bridged organic dipolar molecules consisting of benzene rings with different donor and acceptor groups have been synthesized.[6] The nonlinear optical measurements show a wide variation in magnitudes, depending on the donor and acceptor strengths and their geometrical positions. For a proper understanding of the dependence of nonlinear optical properties on the constituent groups and their geometrical positions in similar groups of structures, we have considered a series of nitroaniline systems where two nitroaniline molecules are connected by a bridged oxygen atom. This oxygen atom can be considered to be acting as a stitch between two nitroaniline molecules. Out of a large number of dinitroaniline configurations, we find that the hyperpolarizability coefficient is maximum for the systems where the molecular dipoles make a 0° angle between them and are on the same plane. However, in reality, these molecular systems are not planar due to steric interactions. Therefore, to put our predictions into maximum applicability, we connect the two nitroaniline rings by a covalent bond. This reduces the nonbonding interaction between the rings and makes them almost planar, thereby giving rise to desired nonlinear optical characteristics.

In the next section we briefly discuss a semiclassical theory based on point dipole interactions. In section 3, we present a theoretical analysis of the nonlinear optical properties of the chromophores as a function of a number of dipolar orientations. This is done using the established ZINDO/CV quantum chemical formalism. We conclude the paper with a summary of all the results.

2. Dipolar Model for the Excitonic Level Splitting

For organic dipolar molecules, the lowest optically allowed energy state is an exciton state, and the interactions between the excitonic states can be expressed in the direct product basis of the chromophoric molecular orbitals if the direct overlap between the chromophoric molecular orbitals is negligible.[7−12] This can be realized only at large distances and thus the coupling between dipolar molecules can be approximated at large distances by a point dipole model. If two molecular species, *m* and *n*, are the same, the coupling interactions can be written as

$$H_{m,n} = \frac{\vec{M}_{ij}\cdot\vec{M}_{ij}}{r_{mn}^{3}} - \frac{3(\vec{M}_{ij}\cdot\vec{M}_{ij})(\vec{M}_{ij}\cdot\vec{r}_{mn})}{r_{mn}^{5}} \qquad (1)$$

where $\vec{M}_{ij}$ is the transition dipole moment from state *i* to state *j* of the monomer molecule and r_{mn} is the distance between the two molecular centers, *m* and *n*. It is to be noted that both the transition dipole and the distance ($\vec{r}_{mn}$) are vectorial quantities. Thus the magnitude of the interaction term will depend crucially on the relative orientations of the dipolar molecules as well as on the axis joining their centers. We shall give here a purely quasi-classical vector treatment to this interaction as we assume electrostatic interaction between the transition moments.[13]

A number of cases can be analyzed considering the dipolar molecules in various orientations. We have considered the oxo-

10.1021/jp030801z CCC: $27.50
Published on Web 12/13/2003

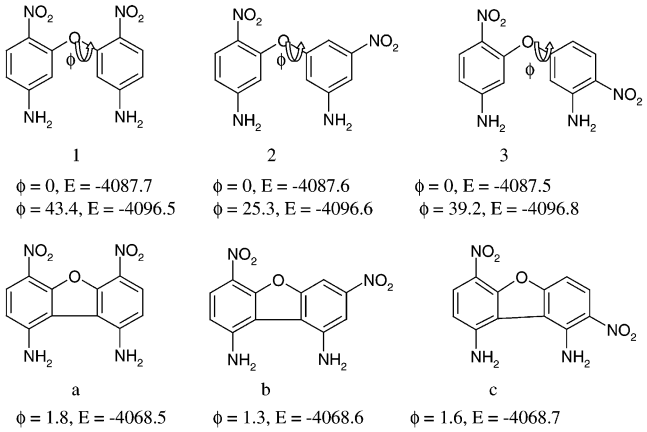

Figure 1. Structures of the three molecules 1, 2, and 3 considered for the quantitative estimations. The energies and twist angle (ϕ) of the systems are indicated. The first row shows the energies (eV) for parallel dipole $\phi = 0°$. The next is for the optimized geometries. (a), (b), and (c) are structures of the rigid molecules fixed by the C−C linkages. Their energies and twist angle (ϕ) are in the last footnote.

bridged dinitroaniline systems as shown in Figure 1. The chromophores are oriented with an angle ϕ between the planes of the molecules and each molecule creates an angle θ with its molecular axis. Twisting of the C−O−C bridge rotates one of the molecule (with an angle ϕ) while fixing the other molecule on the plane. It then becomes quite simple to derive the dipolar splitting energy of the lowest energy excitation

$$\Delta E = 2\frac{M_{gs}^{\ 2}}{r_{mn}^{\ 3}}(\cos\phi - 3\cos\theta_1\cos\theta_2) \qquad (2)$$

where M_{gs} is the transition dipole from the ground state to the excited singlet state of the monomer (excitonic state). Here θ_1 is the angle between the polarization axis and the molecular axis of molecule 1 and θ_2 is the same for the second molecule.

Let us now analyze a few cases with the variance of angles θ_1, θ_2, and ϕ. We keep one of the molecules fixed so that the variance of θ_1 remains zero. Because this fixed molecule is *p*-nitroaniline in our case, θ_1 itself is zero. Now the $(\theta_2, \phi) = (0°, 0°)$ case corresponds to the ideally planar pna−O−pna (paranitroaniline oxo bridged with another paranitroaniline), the case 1 in Figure 1. For the planar pna−O−mna (paranitroaniline oxo bridged with metanitroaniline) and pna−O−ona (paranitroaniline oxo bridged with orthonitroaniline), however, the θ_2 angle is not well-defined. We determine the θ_2 by observing the angle that the dipole moment vector makes with the molecular axes for the optimized geometries of the individual molecules, i.e., 30° and 90° for mna (metanitroaniline) and ona (orthonitroaniline), respectively. Note that this is an approximatation, because in the presence of the bridged oxygen the magnitude of this angle would be different. However, we find that the difference is quite small, and for simplicity we assume the θ_2 values from the individual optimized geometries, i.e., $(\theta_2) = (30°)$ and $(\theta_2) = (90°)$ for pna−O−mna and pna−O−ona (see cases 2 and 3 in Figure 1), respectively. For cases where $(\theta_2, \phi) = (0°, 0°)[(90°, 0°)]$, the electrostatic interaction is attractive [repulsive] in nature for the lowest excited states. Note that the transition moments are finite for electric dipole transitions from the ground state to the state with attractive electrostatic interaction whereas it is vanishing for the states with repulsive interaction.

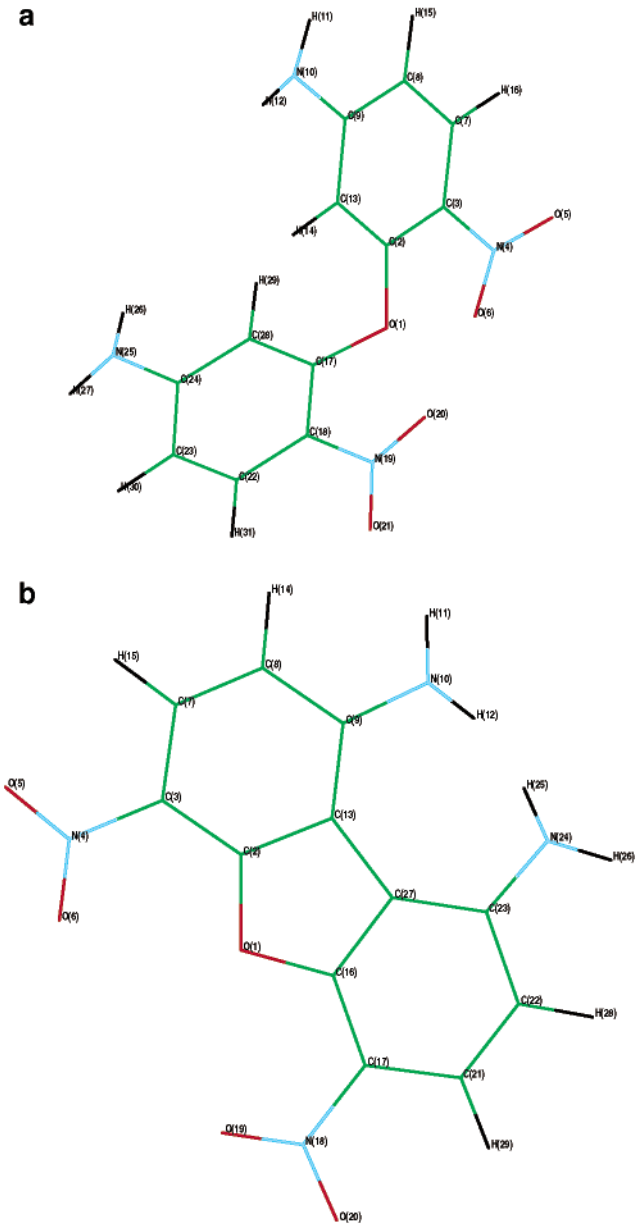

Figure 2. Optimized geometries of pna−O−pna (Figure 2a) and C−C bridged pna−O−pna (Figure 2b). The numbers indicate atomic positions (see Table 1).

3. Results and Discussions

For a quantitative understanding of the phenomenon in general, we carry out extensive numerical calculations of the ground state and the excited states of the oxo-bridged di-nitroaniline systems.

We start our calculations by optimizing the geometries of all the molecules using the semiempirical AM-1 parametrized Hamiltonian without any symmetry constrains[14] available in the Gaussian-98 set of codes.[15] Due to the steric interactions between the nitroaniline rings, the angle connecting the two rings (ϕ) becomes nonzero for the optimized molecules 1, 2, and 3 in Figure 1. The optimized geometry of the pna−O−pna and the C−C bridged pna−O−pna are shown in Figure 2. Their bond lengths and bond angles are shown in Table 1. However, to understand the effects of dipolar orientations on the nonlinear optical properties, we deliberately put the two rings planar and perform single-point energy calculations. We then change the dihedral angle between the two rings by twisting the bond

TABLE 1: Optimized Geometry Parameters[a]

bond length (Å)		angle (deg)	
		pna−O−pna	
C2−O1	1.388	C17−O1−C2	117.2
C17−O1	1.386	C2−C13−C9	120.7
C17−C28	1.416	C13−C9−C8	118.9
C28−C24	1.407	C9−C8−C7	119.8
C24−C23	1.384	C8−C7−C3	121.6
C23−C22	1.418	C7−C3−C2	119.5
C22−C18	1.423	C3−C2−C13	119.5
C18−C17	1.392	C3−N4−O5	119.6
C2−C13	1.398	C3−N4−O6	118.4
C13−C9	1.418	C13−C9−N4	120.3
C9−C8	1.423	C2−01-C17	117.2
C8−C7	1.379	C17−C28−C24	120.4
C7−C3	1.401	C28−C24−C23	118.9
C9−N10	1.374	C24−C23−C22	120.3
C3−N4	1.479	C23−C22−C18	120.7
N4−O5	1.201	C22−C18−C17	119.2
N4−O6	1.203	C18−C17−C28	120.5
C24−N25	1.376	C18−N19−O20	118.3
C18−N19	1.479	C18−N19−O21	119.8
N19−O20	1.204	C24−C23−N25	120.7
N19−O21	1.201	C28−C23−N25	120.5
		pna−O−pna, C−C Bridged	
C2−O1	1.398	C2−O1−C16	105.4
C16−O1	1.397	C16−C27−C23	118.4
C16−C17	1.395	C27−C23−C22	117.4
C17−C21	1.412	C23−C22−C21	122.5
C21−C22	1.382	C22−C21−C17	121.0
C22−C23	1.427	C21−C17−C16	116.8
C23−C27	1.409	C17−C16−C27	123.5
C27−C16	1.432	C2−C3−C7	116.8
C2−C3	1.395	C3−C7−C8	120.8
C3−C7	1.411	C7−C8−C9	122.7
C7−C8	1.383	C8−C9−C13	117.3
C8−C9	1.427	C9−C13−C2	118.4
C9−C13	1.410	C13−C2−C3	117.3
C13−C27	1.459	C8−C9−N10	122.8
C23−N24	1.386	C13−C9−N10	119.9
C17−N18	1.476	O5−N4−O6	122.3
N18−O19	1.198	O20−N18−O19	122.3
N18−O20	1.205	C16−C17−N18	120.5
C3−N4	1.476	C21−C17−N18	122.7
C9−N10	1.386	C7−C3−N4	120.5
N19−O21	1.201	C2−C3−N4	122.7
N4−O6	1.205	H12−N10−H11	114.1
N4−O5	1.198	H26−N24−H25	113.8

[a] Bond length (in angstroms), angles (in degrees) for the pna−O−pna and pna−O−pna bridged by C−C bond (see Figure 2 for the configuration structures).

connecting the bridged oxygen and the carbon in one of the rings. These geometries were used to compute the SCF MO energies and then the spectroscopic properties using the Zerner's INDO method.[16] We use the singles CI (CIS), because the first nonlinear optical coefficients are derived from second-order perturbation theory involving one-electron excitations. The CIS approach adopted here has been extensively used in earlier works and was found to provide excitation energies and dipole matrix elements in good agreement with experiment.[17,18] To calculate nonlinear optical properties, we use the correction vector (CV) method, which implicitly assumes all the excitations to be approximated by a correction vector.[19] Given the Hamiltonian matrix, the ground-state wave function and the dipole matrix, all in CI basis, it is straightforward to compute the dynamic nonlinear optical coefficients. Details of this method have been published in a number of earlier works.[20−22]

Before presenting the nonlinear optical coefficients, we first show the variation of splitting energy (see eq 2) in each case as a function of dihedral angle or the twist angle. The distance between the molecular axis, r_{mn}, was obtained from the geometry of double molecule for the corresponding twist angle, as discussed in the previous paragraph. Figure 3 (upper portion) represents the variation of the modulus of the splitting energy with the variation in ϕ for the three systems 1, 2, and 3 with unit M_{gs}. As can be seen, for molecules 1 and 2, there is almost no variation in splitting energy, whereas for molecule 3, the splitting energy decreases as a function of twist angle, ϕ. Furthermore, the splitting energy is negative for cases 1 and 2, whereas it is positive for case 3. However, in all the cases the absolute value of the splitting energy is quite small.

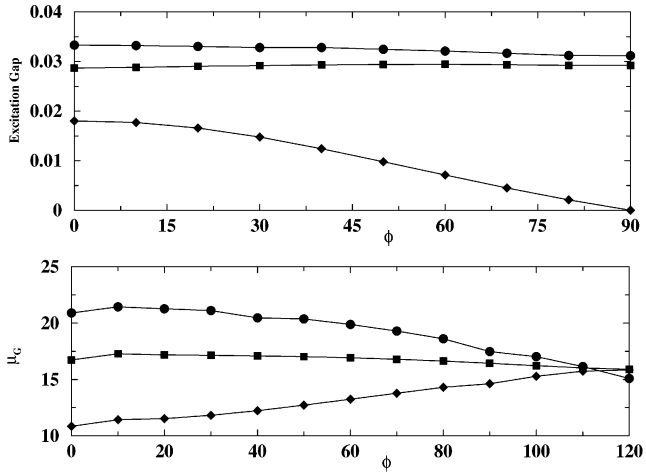

Figure 3. (Upper panel) variation of the magnitude of the splitting energy (eV) as a function of the dihedral angle for the three systems 1 (●), 2 (■), and 3 (◆). (Lower panel) variation of the ground-state dipole moment μ_G (Debye), as a function of the dihedral angle for the same three systems.

In the lower panel of Figure 3, we plot the total ground-state dipole moment μ_G (in Debye) for these three systems as a function of angle ϕ. We find that though the dipole moment decreases with increase in ϕ for cases 1 and 2, it increases for case 3. This can be easily understood by considering the combined effects of ground-state dipoles in each cases. If the two dipoles are parallel and in the same plane, the in-phase combination of the resultant dipole is the sum of the two individual dipoles. For the pna−O−ona (case 3), the two dipoles are pointing almost perpendicular to each other when they are in the same plane ($\phi = 0°$ limit). Thus their in-phase combination gives a very small net total dipole moment, μ_G. However, as ϕ increases from zero, the angle between the two dipoles reduces, increasing the in-phase combination of the total dipole moment (or equivalently, reducing the out-of-phase combination). Thus the μ_G increases with increasing ϕ for pna−O−ona. However, for pna−O−pna (case 1) and for pna−O−mna (case 2), the $\phi = 0°$ configuration is the most favorable orientation in terms of their total ground-state dipole moment. As ϕ increases from zero, the monomer dipoles rather oppose each other, the in-phase combination of which reduces the μ_G.

To firmly establish the above qualitative discussions, we present in Figure 4, the relative phases of the constituent molecules forming the dimer for the pna−O−pna cases. The ground and the lowest optically excited states are shown for pna−O−pna parallel dipoles ($\phi = 0°$), the optimized geometry, and the rigid molecule with C−C linkage (structure *a* in Figure 1). The ground state (HOMO level) is an even-parity combination of the atomic orbitals from the individual rings, whereas for the LUMO level (the lowest optically active single excitation), the combination is out-of-phase or antisymmetric. From the figures, it is quite clear that with an increase in ϕ, the

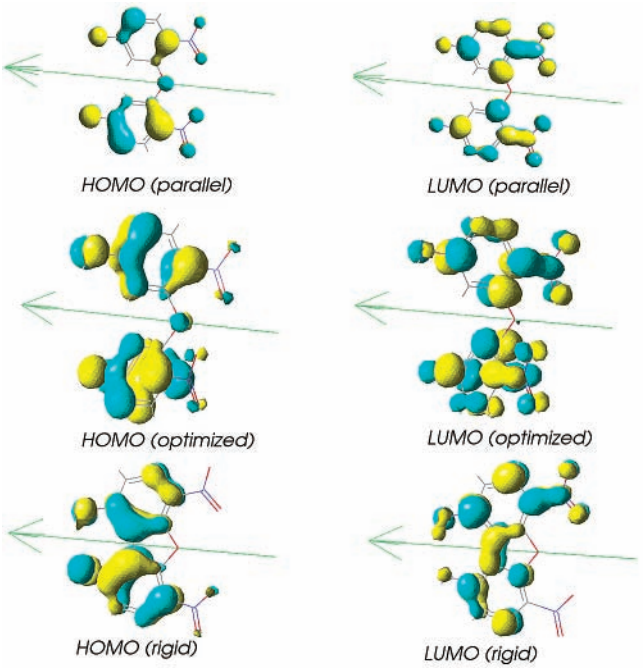

Figure 4. AM1-derived HOMO and LUMO molecular orbitals for (first row) the parallel dipoles ($\phi = 0°$) for pna−O−pna, (second row) the optimized geometries, and (third row) rigid pna−O−pna connected by a C−C linkage. The shading represents the phase of the wave functions. The arrows indicate the directions of the dipole moments.

magnitude of μ_G as well as the electric transition dipoles would reduce. In the MO picture, the electric field connects the ground state to a state with exactly opposite parity. The transition dipole strength will be a maximum for the case where the change in parity is complete (even to odd) on going from the HOMO to LUMO. Because the HOMO level for $\phi = 0°$ pna−O−pna has the best in-phase combination (phase difference is zero), the μ_G is highest for this case. On the other hand, for the optimized pna−O−pna geometry, the phase difference is 43.4°, which accounts for the small μ_G in this case. For the rigid geometry, however, the phase combination in the HOMO level is almost symmetric (phase difference ~1.8), together with a notable contribution from the C−C bond although the dipoles are very close to being parallel. The phase difference in the HOMO level together with the parity difference between the HOMO and the LUMO level would account for the EFISHβ values found in various geometries, discussed later.

The bridged oxygen atom does not play any significant role in determining the nonlinear optical coefficients. It basically controls the distance between the two nitroaniline dipoles. Due to its high electronegativity, it just increases the total dipole moment of the dimeric systems (it increases roughly 1 D purely because of oxygen) to the same extent for all values of the dihedral angle, ϕ. Thus, even though our semiclassical theory of dipole−dipole interaction does not take into account the electronic properties of the bridged O atom, we find that the qualitative trend in splitting energy as a function of the angle ϕ is almost the same with those obtained from CIS calculations for the di-nitroaniline systems.

For the calculations of the optical coefficients, we have used 1064 nm (1.17 eV) as the excitation frequency of the oscillating electric field which corresponds to the frequency of the Nd:YAG lasers used in experiments. We plot the variation in EFISH (electric field induced second harmonic) coefficients with the angle ϕ in Figure 5. The trend is very similar to that for the ground-state dipole moment in Figure 3. To be precise, the

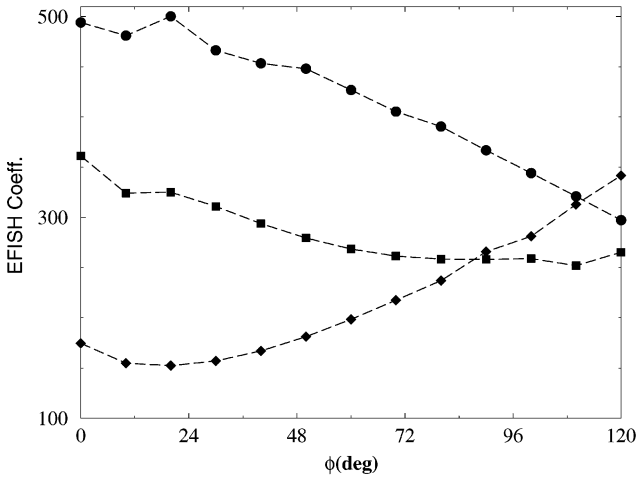

Figure 5. Plot of the EFISH coefficients (10^{-30} esu × Debye), as a function of the dihedral angle for the three systems 1 (●), 2 (■), and 3 (◆). The input electric field frequency in all cases is 1.17 eV.

magnitude of EFISH coefficient decreases with an increase in the torsional angle for the pna−O−pna and for the pna−O−mna, whereas for the pna−O−ona, the magnitude of the same increases. Within the framework of the two-state model, the second harmonic generation (SHG) response can be written as[23]

$$\beta_{\text{two-level}} = \frac{3e^2}{2\hbar} \frac{\omega_{12} f \Delta\mu_{12}}{(\omega_{12}^2 - \omega^2)(\omega_{12}^2 - 4\omega^2)} \qquad (3)$$

where $\hbar\omega_{12}$ is the excitation energy, f is the oscillator strength, $\Delta\mu_{12}$ is the difference between the dipole moments of the ground and the excited state, and ω specifies the excitation frequency of the oscillating electric field. This simple expression tells us that β will increase (decrease) if ω_{12} is small (large) and μ and f are large (small).

The EFISH coefficients shown in Figure 5 are the product of dipole moment (μ) and the SHG coefficients (β). β is computed as the tumbling average quantity, defined as $\beta = {}^1/_3(\beta_{xyy} + \beta_{yyx} + \beta_{yxy})$. From Figure 3 (upper panel), it is clear that for pna−O−pna and for pna−O−mna, the energy difference between the ground and the one-photon state remains almost constant as a function of the torsional angle, ϕ. Thus, for these two systems, there is a very negligible effect of splitting energy on the magnitude of β. This suggests that the β values can be tuned to a large extent according to the ground-state dipole moment, if the oscillator strength is appreciable. This is precisely the EFISH coefficients trend observed for systems 1 and 2, as a function of ϕ. For pna−O−ona, however, the EFISH coefficient increases with the increase in the angle ϕ. Interestingly, for this case, with the variation of ϕ, the increase in the ground-state dipole is not much; the reduction in energy gap between the ground state and the one-photon state decides the trend for the EFISH coefficients.

We shall ask the question now as to how is it possible to achieve such high EFISH coefficients with desired dipole orientations in optimized oxo-bridged dinitroaniline systems. The highest EFISH coefficients (494.4×10^{-30} esu) are obtained for pna−O−pna with zero dihedral angle. Such a high value of EFISH coefficient cannot be realized for the real molecular system, as the optimized geometries of the dinitroaniline molecules discussed above are not planar due to steric repulsions. Therefore, our best suggestion is to connect the oxo-bridged rings by a carbon−carbon bond in the meta position. Optimizations of the structures, (a) and (b) in Figure 1, by the

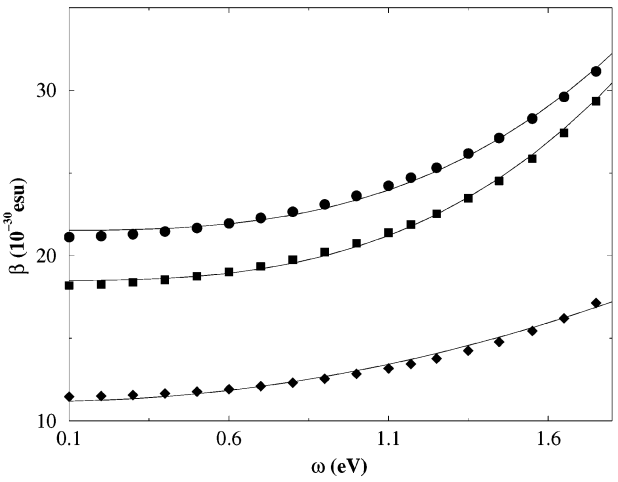

Figure 6. Dispersion curves for β (10^{-30} esu) for rigid configurations as in Figure 1: a (●); b (■); c (◆). The frequency is in electronvolts.

same method described earlier confirm that the nitroaniline rings are almost planar with the dihedral angle ϕ very close to zero. Thus one can make the two dipoles to be parallel to a large extent by bridging the two rings by a covalent bond. For case c, however, the optimized geometry is not planar. The rings themselves twist in the optimized structure of (c). This is due to the steric repulsion among the closely spaced three groups (see Figure 1c).

The EFISH coefficients for the optimized geometry of (a) is 471.5×10^{-30} esu, close to the parallel ($\phi = 0°$) pna−O−pna dipole value. For the pna−O−mna cases, the values for parallel dipoles ($\phi = 0°$), and the optimized structure (b) are 307.8×10^{-30} and 301.6×10^{-30} esu, respectively. Thus we can safely conclude that the C−C connected dipole provides a better choice of materials. However, for the pna−O−ona systems, we find some different results. The values for parallel dipoles ($\phi = 0°$), and the optimized structure (c) are 147.7×10^{-30} and 77.6×10^{-30} esu, respectively. From Figure 5, we see that EFISH coefficient is lowest for case 3 (Figure 1) when the dihedral angle is zero and its magnitude increases with an increase in ϕ. Thus we expect the optimized structure (c) to give high values of EFISH coefficients compared to those of $\phi = 0°$, case 3 (Figure 1). However, as we see, the magnitude is quite small. We attribute such a low value of the EFISH coefficient to the following. The C−C covalent connection would try to keep the rings planar; however, this would force three groups (two NH_2 and one NO_2) to come close to each other. This results in strong steric repulsions, and as a result, the two NH_2 groups bend away from the plane of the benzene rings. Consequently, the π electron delocalization length decreases, decreasing the EFISH coefficient to a large extent.

Our results compare fairly well with the experimental values. For example, we have calculated the β for the optimized bis-(2-amino-4-nitrophenyl) ether, for which the experimental β value from hyper-Rayleigh scattering (HRS) experiments at the Nd:YAG frequency is 22.0×10^{-30} esu,[6] whereas our estimate at the same frequency gives $\beta = 16.4 \times 10^{-30}$ esu.

Next we consider the dispersion relation for the first nonlinear polarizability coefficients (β). Because this needs to be done for a fixed geometry, we consider the optimized geometries of C−C connected oxo-bridged dinitroaniline compounds (a), (b), and (c), as in Figure 1. The dispersion relations for β are shown in Figure 6. The magnitude of β coefficients increases rapidly with the increase in ω for all three cases. However, for (a) and (b), the increase of β is cubic in ω, $\beta = A + B\omega^3$, and for (c), it is quadratic, $\beta = C + D\omega^2$. The lowest one-photon excitation gap for these molecules are of the order of 4.0 eV, and so we have carried out the β computations up to $\omega \sim 1.8$ eV, well below the resonance frequency. From this, we can safely conjecture that although the C−C bonded pna−O−pna and pna−O−mna compounds are good candidates for optical rectification, the corresponding pna−O−ona is not.

To conclude, we have carried out extensive semiempirical calculations of nonlinear optical coefficients on a few dipolar organic molecules in a number of their dipolar configurations. Although our results are based on semiempirical computations, the results have been verified with varying number of CIs. We find that the ground-state dipole moment and the hyperpolarizability are governed by the extent of π-electron delocalization, which in turn depends on the structural details of the molecules. On the basis of our calculations, we have proposed molecular systems where large magnitudes of first-order hyperpolarizabilities can be realized. From a synthesis point of view, these molecules are rather simple to prepare; analogous systems have been synthesized with good yield.[6] Therefore, we believe that a synthetic scheme well suited for the best dipolar arrangements can be fine-tuned to obtain large nonlinear optical properties at extremely low-energy.

Acknowledgment. One of us (S.K.P.) thanks Council of Scientific and Industrial Research (CSIR), Govt. of India, for the research grant.

References and Notes

(1) Prasad, P. N.; Williams, D. J. *Introduction to Nonlinear Optical Effects in Molecules and Polymers*; Wiley: New York, 1991.

(2) *Polymers for Second-Order Nonlinear Optics*; Lindsay, G. A., Singer, K. D., Eds.; ACS Symposium Series 601; Washington, DC, 1995.

(3) Marks, T. J.; Ratner, M. A. *Angew. Chem., Int. Ed. Engl.* **1995**, *34*, 155.

(4) *Optical Nonlinearities in Chemistry*; Burland, D. M., Ed. *Chem. Rev.* **1994**, *94*, 1.

(5) Williams, D. J. *Angew. Chem., Int. Ed. Engl.* **1984**, *23*, 690.

(6) Sudharsanam, R.; Chandrasekaran, S.; Das, P. K. *J. Mol. Struct.* **2003**, *645*, 51.

(7) Davydov, A. S. *Theory of Molecular Excitons*; McGraw-Hill: New York, 1962.

(8) Suzuki, H. *Electronic Absorption Spectra: Geometry of Organic Molecules*; Academic Press: New York, 1967.

(9) Harada, N.; Takuma, Y.; Uda, H. *J. Am. Chem. Soc.* **1978**, *100*, 4029.

(10) *Circular Dichroic Spectroscopy: Exciton Coupling in Organic Stereochemistry*; Nakanishi, K., Ed.; University Science Books: Mill Valley, CA, 1983.

(11) Scholes, G. D.; Ghiggino, K. P.; Oliver, A. M.; Paddon-Row, M. N. *J. Am. Chem. Soc.* **1993**, *115*, 4345.

(12) McCullough, J. *Chem. Rev.* **1987**, *87*, 811. Kasha, M. *Rev. Mod. Phys.* **1959**, *31*, 162.

(13) Datta, A.; Pati, S. K. *J. Chem. Phys.* **2003**, *118*, 8420.

(14) Dewar, M. J. S.; Zoebisch, E. G.; Healy, E. F.; Stewart, J. J. P. *J. Am. Chem. Soc.*, **1985**, *107*, 3902.

(15) Frisch, M. J.; Trucks, G. W.; Schlegel, H. B.; Scuseria, G. E.; Robb, M. A.; Cheeseman, J. R.; Zakrzewski, V. G.; Montgomery, J. A., Jr.; Stratmann, R. E.; Burant, J. C.; Dapprich, S.; Millam, J. M.; Daniels, A. D.; Kudin, K. N.; Strain, M. C.; Farkas, O.; Tomasi, J.; Barone, V.; Cossi, M.; Cammi, R.; Mennucci, B.; Pomelli, C.; Adamo, C.; Clifford, S.; Ochterski, J.; Petersson, G. A.; Ayala, P. Y.; Cui, Q.; Morokuma, K.; Salvador, P.; Dannenberg, J. J.; Malick, D. K.; Rabuck, A. D.; Raghavachari, K.; Foresman, J. B.; Cioslowski, J.; Ortiz, J. V.; Baboul, A. G.; Stefanov, B. B.; Liu, G.; Liashenko, A.; Piskorz, P.; Komaromi, I.; Gomperts, R.; Martin, R. L.; Fox, D. J.; Keith, T.; Al-Laham, M. A.; Peng, C. Y.; Nanayakkara, A.; Challacombe, M.; Gill, P. M. W.; Johnson, B.; Chen, W.; Wong, M. W.; Andres, J. L.; Gonzalez, C.; Head-Gordon, M.; Replogle, E. S.; Pople, J. A. *Gaussian 98*, revision A.10; Gaussian, Inc.: Pittsburgh, PA, 2001.

(16) Ridley, J.; Zerner, M. C. *Theor. Chim. Acta* **1973**, *32*, 111. Bacon, A. D.; Zerner, M. C. *Theor. Chim. Acta* **1979**, *53*, 21.

(17) Buenker, R. J.; Peyerimhoff, S. D. *Theor. Chim. Acta* **1974**, *35*, 33. Shuai, Z.; Beljonne, D.; Bredas, J. L. *J. Chem. Phys.* **1992**, *97*, 1132.

(18) Albert, I. D. L.; Marks, T. J.; Ratner, M. A. *J. Phys. Chem. A* **2000**, *104*, 837.

(19) Ramasesha, S.; Soos, Z. G. *Chem. Phys. Lett*. **1988**, *153*, 171. Soos, Z. G.; Ramasesha, S. *J. Chem. Phys*. **1989**, *90*, 1067.

(20) Ramasesha, S.; Shuai, Z.; Bredas, J. L. *Chem. Phys. Lett*. **1995**, *245*, 224. Albert, I. D. L.; Ramasesha, S. *J. Phys. Chem*. **1990**, *94*, 6540. Ramasesha, S.; Albert, I. D. L. *Phys. Rev. B* **1990**, *42*, 8587.

(21) Pati, S. K.; Ramasesha, S.; Shuai, Z.; Bredas, J. L. *Phys. Rev. B* **1999**, *59*, 14827.

(22) Pati, S. K.; Marks, T. J.; Ratner, M. A. *J. Am. Chem. Soc*. **2001**, *123*, 7287.

(23) Oudar, J. L.; Chemla, D. S. *J. Chem. Phys*. **1977**, *66*, 2664. Oudar, J. L. *J. Chem. Phys.* **1977**, *67*, 446.